On the Mechanism of Hydrodynamic Reinforcement in Elastic Composites

Gregor Huber‡ and Thomas A.Vilgis*,†

Max-Planck-Institut fur Polymerforschung, Postfach 3148 D-55021 Mainz, Germany; and Bayer AG, 51368 Leverkusen, Germany

Received June 11, 2002; Revised Manuscript Received August 15, 2002

ABSTRACT: We present recent results of theoretical investigations concerning the hydrodynamic reinforcement contribution in different elastic composite systems: elastic matrix plus (i) rigid filler particles with fractal structure (e.g., carbon black aggregates); (ii) spherical core−shell particles with soft core and hard shell; (iii) spherical core−shell particles with hard core and soft shell (e.g., carbon black particles with bound rubber). Detailed predictions are made on the resulting modulus of the composite systems.

I. Introduction

Reinforcing rubbers and other elastic nanocomposite materials[1] is an open problem from the theorist's point of view. The mechanisms of the effective enhancement of the elastic modulus cannot be understood by one simple theory, since several interactions and many different length scales are involved.[2] This has its reason in the different physical levels of reinforcement. The rubber matrix contributes by rubber elasticity,[4] whereas the presence of filler particles contributes by different mechanisms. Most well-known are volume effects, also called hydrodynamics interactions (due to the analogy of the enhancement of the viscosity of liquids by the addition of particles).

In the context of carbon black filled elastomers, the contribution to reinforcement on small scales can be attributed to the complex structure of the branched filler aggregates as well as to a strong surface polymer interaction, leading to the so-called bound rubber. Thus, the filler particles are coated with polymer chains, and the binding (physically or chemically) of elastomer chains to the surface of the filler particles changes the elastic properties of the macroscopic material significantly.[3] On larger scales the hydrodynamic aspect of the reinforcement dominates the physical picture. Hydrodynamic reinforcement of elastic systems plays a major role not only in carbon black filled elastomers but also in composite systems with hard and soft inclusions. Finally, at macroscopic length scales, the existence of filler networking at medium and high filler volume fractions plays the dominate role. The major results on these issues can be already found in ref 2.

In this paper we are going to concentrate—on a general basis—on the different mechanisms of elastomer reinforcement in the hydrodynamic regime. To do so, we present two different regimes of reinforcement mechanisms. To introduce the subject, we dwell briefly on the classical ideas. The simplest approach was presented as early as 1944 by Smallwood,[5] where it was shown that adding randomly dispersed, spherical filler particles to a rubbery matrix yields an elastic reinforcement of the form

$$E = E_m(1 + 2.5\phi) \tag{1.1}$$

This is known as the Einstein−Smallwood formula, where ϕ is the volume fraction of the filler components and E_m denotes the elastic modulus of the matrix. The physical conditions for this result are as follows: (i) freely dispersed particles, i.e., low volume fraction, (ii) spherical shape (leading to the constant 2.5), and (iii) entirely nonelastic filler particles, i.e., where their elastic modulus has to be infinitely large. Although the assumptions are very strict and idealized, the Einstein−Smallwood equation contains very essential physics. The reinforcement term contains two factors: one is a simple number which is related only to the geometry of the particles; the other is linear in the volume fraction of the filler particles. This latter point corresponds to a more general physical principle, as we are going to see later. As long as the filler particles do not overlap, this term will stay linear in this expansion.

In real systems none of these assumptions is valid rigorously, and many authors have provided generalizations of eq 1.1 by relaxing some of the conditions (i−iii). For example particle−particle interaction at less low filler volume fraction can be taken into account by an additional term quadratic in ϕ, which was first done by Guth and Gold.[6] But most of these extensions have been carried out on a highly empirical basis. Here we want to show that interesting generalizations can also be attained by rigorous theoretical calculations, thereby illuminating the main mechanisms of hydrodynamic reinforcement in complex composite systems.

In this paper we are going to present two other extremes cases and shed light on the principal issues of the Einstein−Smallwood theory. First we are going to generalize on the dispersion of the filler particles. As mentioned above, the linear dependence in eq 1.1 stems basically from the assumption of free dispersion of the filler particles. Only in this case are the conditions for an expansion in terms of the volume fraction given. If the filler particles form clusters, two different regimes must be distinguished. First, small clusters may be dispersed freely without contacts between them. Then we can expect, that a reinforcement law as given by

* Corresponding author.
† Bayer AG.
‡ Max-Planck-Institut fur Polymerforschung.

10.1021/ma0208887 CCC: $22.00
Published on Web 10/26/2002

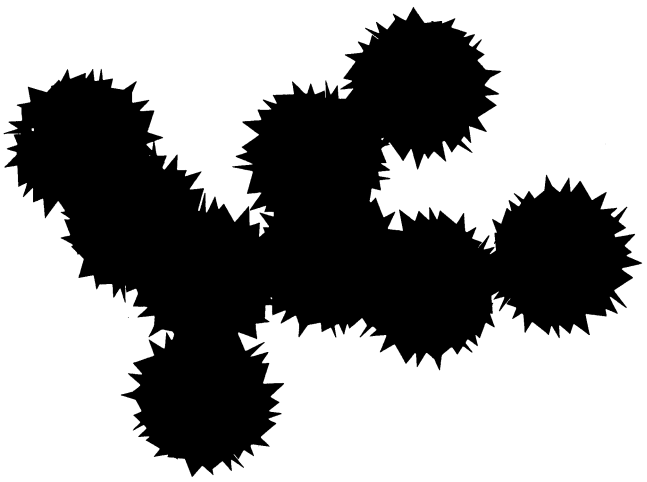

Figure 1. Schematic view of the carbon black aggregate structure, which can be characterized by fractal exponents.

Einstein−Smallwood holds. The only changes can be expected in the geometry factor, which may become size dependent. The second regime comes into play when the clusters begin to overlap. Then a different behavior as a function of the volume fraction ϕ can be expected. If it is assumed that the clusters may have some "fractal" geometry, some scaling relations are derived below. In the overlap regime a stronger reinforcement is expected.

The other extreme generalization of the Einstein−Smallwood law will assume not only gain-free dispersion but also filler particles with more complex elastic properties. In this part of the paper, we will present a detailed theory on so-called core shell systems. To do so, we assume the shape of the filler particles again as spherical, but they may have, e.g., a hard core of a different elastic modulus and a softer shell. The second assumption in this part of the paper is that these core shell filler particles are distributed randomly in the elastic matrix; i.e., we assume they do not cluster. Alternatively the theory is kept general, so that also filer particles with holes ("swiss cheese"-like solids) can be discussed.

II. Rigid Filler Aggregates with Fractal Structure

A. General Remarks. Deviations from the Einstein−Smallwood formula for nonspherical filler particles, e.g., carbon black aggregates, so far have mostly been discussed in terms of an effective volume fraction $\phi_{\text{eff}} > \phi$[7,8] while retaining the form of eq 1.1. Carbon black aggregates are built up from approximately spherical primary particles which are connected in a branched but nevertheless solid way; see Figure 1. These structures are known to have universal features and thus can be characterized by the fractal exponents d_f (mass fractal dimension) and D (spectral dimension as a measure of aggregate connectivity).[7,9]

The branched aggregate structure leads to the possibility of aggregate overlap in the case of medium and high filler volume fractions. We expect this to affect not only the factor ϕ_{eff} but also the scaling behavior of the ϕ dependence. Therefore, we use an elastic theory to calculate—independent of the Einstein−Smallwood formula—the dependence of the modulus on the universal fractal structure of carbon black aggregates.[2] The calculations, however, are nontrivial and require methods known from effective medium theories,[10,11] The mathematical formalism requires some ideas from the general theory of Green functions. Indeed the formalism presented in refs 10 and 11 can be extended to more general shapes of fractal filler agglomerates (or filler clusters of a certain shape which satisfies on reasonable scales certain scaling relations regarding their size and their connectivity). The filler particles which have a certain shape interact with the elastic matrix and eventually at larger concentrations than the overlap concentration with themselves. For the small deformations considered here, we can assume a perfect binding of the matrix to the filler surfaces. Furthermore, the interaction between filler aggregates is not taken into account explicitly, the matrix is considered as incompressible and ideally elastic. The many particle effects which occur at higher concentrations are dealt with in the framework of an effective medium theory, the so-called "self-consistent screening approximation".[11,12] We are not going to present their outline in the main text but in Appendix A at the end of this paper.

B. Fractal Aggregates. To pursue studies with the model, we have to extract from the general result derived in appendix A the modulus of reinforcement for fractal-shaped fillers. We may assume that the clusters formed by the filler particles can be described by a fractal shape. We do so only to describe the structure, rather than to suggest that the structure *is* fractal. It will be obvious shortly below that this assumption allows one to predict certain specific forms of the reinforcement. First this allows one to introduce an effective probability distribution for the filler clusters as[13,14]

$$P[\mathbf{R}(s)] \sim \exp\left\{-\frac{3}{2b^2}\int_0^L \mathrm{d}^D s \left(\frac{\partial \mathbf{R}(s)}{\partial s}\right)^2\right\} \qquad (2.1)$$

$$\sim \exp\left\{-\frac{3}{4\pi b^2}1\sum_{\mathbf{p}}|\mathbf{p}^2|\mathbf{R}_{\mathbf{p}}|^2\right\} \qquad (2.2)$$

where b is the size of the individual filler particles (primary particle). The spectral dimension D describes the connectivity of the filler particle, e.g., linearly connected objects such as polymer chains or random walks correspond to $D = 1$, percolation clusters roughly to $D = {}^4/_3$. $\mathbf{R}(s)$ describes any spatial vector which points on the object. For our purpose, it is useful to work in Fourier space. Therefore, we introduce the transform $\mathbf{R}(s) = \sum_{\mathbf{p}}\mathbf{R}_{\mathbf{p}}\exp(i\mathbf{s}\cdot\mathbf{p})$ by analytic continuation for arbitry spectral dimensions. Thus, $\mathbf{p}$ is the Fourier conjugate to the internal space variable $\mathbf{s}$.

However, the modeling of the filler structure needs a further generalization to self-avoidance. In this case, we may generalize the distribution to[14] through

$$P[\mathbf{R}(s)] \sim \exp\left\{-\frac{3}{4\pi b^2}\sum_{\mathrm{p}}\mathbf{p}^{2\alpha}|\mathbf{R}_{\mathrm{p}}|^2\right\} \qquad (2.3)$$

where $\alpha = D(2 + d_f)/2d_f$. This Gaussian distribution results from a coarse graining which produces a structure similar to the case of branched polymers with excluded volume; see Figure 2. Note that for the choice of $D = 1$ and $d_f = 2$, the above equation reduces to the probability distribution of random walks shaped curves.

The effective exponent $\alpha \neq 1$ can be expressed in terms of the corresponding fractal dimensions, i.e., $\langle \mathbf{R}^2 \rangle \sim L^{2\alpha-D} \sim L^{2\nu}$ or $d_f = 2D/(2\alpha - D)$ yields $\alpha = \nu + D/2$ or

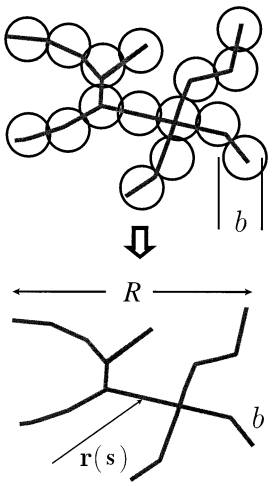

Figure 2. Coarse graining of the filler aggregate structure, leading to a mathematical description similar to the case of branched polymers with excluded volume. b denotes the mean primary particle diameter and R the mean aggregate size.

alternatively with the excluded volume exponent $\nu = D/d_f = 2/d_w$. Furthermore, we note the more general relations (see ref 14 for review) $\nu = 2 - D/2$ for ideal phantom clusters (where the branches could penetrate) and, more realistically, clusters with excluded volume $\nu = (D + 2)/(d + 2)$. The next step is to calculate the self-energy function (see Appendix A), which corresponds directly to the reinforcement factor. First we note that the shape function has the general form

$$\langle \phi^2(\mathbf{k},q)\rangle \sim \frac{(kb)^{(2-D)/\nu}}{(k^2b^2C_1)^{1/\nu} + q^2} \tag{2.4}$$

which is easily calculated by the use of the distribution equation eq 2.3 and the decomposition in "Rouse modes". Then the self-energy can be written as

$$\Sigma(\mathbf{k}) \sim c(kb)^{(2-D)/\nu} \sum_q \frac{\{K(q)\}^{-1}}{(k^2b^2C_1)^{1/\nu} + q^2} \tag{2.5}$$

where c is the filler concentration and C_1 a numerical factor. Equation 2.5 can be evaluated further and yields different results for the overlap and nonoverlap regimes. To see this the evaluation of the self-energy has to be analyzed for the overlap criterium according above the overlap concentration $c \sim N/R^3$, where N is the number of primary particles of size b in the cluster and R its average extension. The clusters overlap only if their connectivity is not too large. We have worked out criteria for these conditions in.[15,16] It was shown that the spectral dimensions should not exceed $^6/_5$ for ideal and $^4/_3$ for nonideal clusters. Clusters with larger connectivities do no longer overlap significantly. Then the self-energy can be written as

$$\Sigma(k) \underset{k\to 0}{\sim} \begin{cases} c\mu b^{-2}(kb)^{(2-D)/\nu}L^{2+\nu-2D} & \text{without overlap: } \xi \geq bL^\nu \\ c\mu b^{-2}(kb)^{(2-D)/\nu}L^{2-D}(\xi/b)^{1-(D/\nu)} & \text{with overlap: } \xi \ll bL^\nu \end{cases} \tag{2.6}$$

where L is the mean (linear) cluster diameter.

C. Screening Lengths. The last step in our approach is the computation of the screening length which will introduce the cluster concentration (or volume fraction). The screening length can be estimated by simple scaling arguments and alternatively by the use of the general theory outlined in Appendix A. Both methods yield the same results and we restrict ourselves to present the scaling estimates.

To do so, we note that the overlap concentration for the clusters is given by

$$c^* = \frac{b^3L^D}{R^3} = \frac{b^3L^D}{b^3L^{3\nu}} = L^{D-3\nu} \tag{2.7}$$

and assume that the screening length has (as in the theory of polymer solutions) the simple scaling form

$$\xi = Rf\left(\frac{c}{c^*}\right) = R\left(\frac{c}{c^*}\right)^x = bL^\nu\left(\frac{c}{c^*}\right)^x \tag{2.8}$$

Simple geometrical arguments and dimensional counting yield the result

$$\xi = \begin{cases} bc^{1/(d_f-3)} = bc^{\nu(D-3\nu)} & \text{general} \\ bc^{-(2-D)/(6-5D)} & \text{for ideal clusters } D < 6/5 \\ bc^{-(D+2)/2(3-D)} & \text{for swollen clusters} \end{cases} \tag{2.9}$$

The scaling results can be confirmed by the calculation of the self-energy, and we simply remark this by the result

$$\Sigma(\boldsymbol{k}) \sim c\mu b^{-2}(\xi/b)^{1-(D/\nu)} \tag{2.10}$$

where ξ must be of the same form as predicted by the scaling arguments, since we must have $\Sigma \sim \mu\xi^{-2}$.

D. Reinforcement by Fractal Aggregates. These results allows one to predict the reinforcement factor as a function of the volume fraction $\phi = b^3c$. To bring the results in a more useful form we replace the linear cluster size L by its spatial dimension $R = bL^\nu$ in eq 2.6. Together with $G_0(\mathbf{k}) \sim \mu^{-1}k^{-2}$, we receive the general result

$$\frac{E - E_m}{E_m} \underset{k\to 0}{\sim} (kb)^{(2-2\nu-D)/\nu} \times \begin{cases} \left(\frac{R}{b}\right)^{(2+\nu-2D)/\nu} c & \text{below overlap concentration} \\ \left(\frac{R}{b}\right)^{(2-D)/\nu} c2\nu/(3\nu-D) & \text{above overlap concentration} \end{cases} \tag{2.11}$$

or alternatively by use of $\nu = D/d_f$

$$\frac{E - E_m}{E_m} \underset{k\to 0}{\sim} (kb)^{2(d_f/D)-2d_f-2} \times \begin{cases} \left(\frac{R}{b}\right)^{2(d_f/D)-2d_f+1}\phi & \text{no overlap } \phi \leq \left(\frac{R}{b}\right)^{d_f-3} \\ \left(\frac{R}{b}\right)^{2(d_f/D)-d_f}\phi & \text{with overlap } \phi \gg \left(\frac{R}{b}\right)^{d_f-3} \end{cases} \tag{2.12}$$

For the case of a realistic modeling of carbon black aggregates by diffusion-limited aggregation (DLA) clus-

ters[7,9] with $d_f \approx 2.5$ and $D \approx {}^4/_3$, we find

$$\frac{E - E_m}{E_m} \sim \begin{cases} R^{-1/4}\,\phi & \text{for } \phi < \phi_c \text{ (a)} \\ R^{5/4}\,\phi^4 & \text{for } \phi > \phi_c \text{ (b)} \end{cases} \qquad (2.13)$$

$\phi_c = (R/b)^{-1/2}$ denotes a critical overlap volume fraction for the branched filler aggregates. Thus, the two different regimes correspond to (a) nonoverlapping clusters and (b) overlapping clusters, depending on filler volume fraction. In the nonoverlapping regime, the behavior is similar to eq 1.1 as we had guessed earlier; i.e., the reinforcement is proportional to the volume fraction whereas in regime b the hydrodynamic reinforcement sensitively depends on the universal aggregate structure.

In the nonoverlapping regime (a), the filler contribution to the modulus is always proportional to the filler concentration itself and a geometrical factor. Because of the fractal nature of the filler aggregates, this factor here depends on the mean aggregate size. This stems from the general concept of fractal elasticity.[9] From eq 2.13, we determine the aggregate size dependence of the reinforcement to be weak without overlap, but almost linear with overlap. This again is a result of the branched structure of the filler aggregates. Disadvantages of this model are the small range of application and the idealizations which we introduced in order to make the calculations tractable. Advantages are the successful derivation of a structure−property relationship, the possibility to explicitly include the fractal filler structure, and the universality (transfer to all types of branched aggregates). Refinements of the present model require the inclusion of the local properties, such as particle−particle binding between the primary filler particles.

In summary, the dependence of the hydrodynamic reinforcement contribution on the universal aggregate structure is found to be weak at small filler concentration, but very strong for high filler content. Similar results have been found and confirmed by experimental data in ref 17.

III. Core−Shell Systems

In the next step, we return to spherical filler particles but relax the condition of filler particle stiffness. Thus, we assume that the particles still are freely dispersed but have themselves elasticity. Examples for such filler particles are elastic microgels or latices. The general theory for such systems has already been derived by Felderhof and Iske,[18] where the theoretical details can be found. Their general result for the effective shear modulus is

$$\frac{E}{E_m} = 1 + \frac{[\mu]\phi}{1 - \frac{2}{5}[\mu]\phi} \qquad (3.1)$$

This results from a mean field approximation, which corresponds to the Lorentz local field method in the theory of dielectrics, leading to the famous Clausius−Mosotti equation for the effective dielectric constant. For rigid and spherical filler particles at low volume fraction, the Einstein−Smallwood formula is recovered because of $[\mu] = {}^5/_2$ (the intrinsic modulus $[\mu]$ follows from the solution of a single-particle problem). But the result clearly goes beyond the limits of Einstein−Smallwood, since two-body interaction (excluded volume) is included, leading to the strong increase of the modulus at high volume fraction.

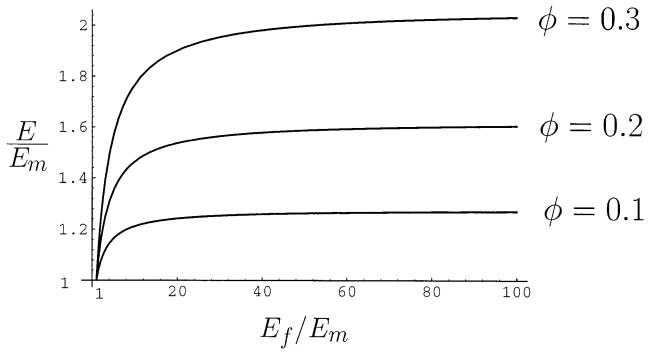

Figure 3. Uniform soft filler particles with elastic modulus E_f: relative increase of the elastic modulus as a function of the ratio E_f/E_m for different values of the filler volume fraction.

Thus eq 3.1 provides an useful frame for the investigation of specific composite systems with spherically symmetric filler geometry: only the intrinsic modulus $[\mu]$ remains to be calculated. Along the lines of Jones and Schmitz,[19] this can be done from the hydrostatic equilibrium equation for one particle included in a continuous elastic medium. In general, the equilibrium equation can be solved only numerically. Exact analytical results are obtained in the following cases.

A. Uniform Soft Sphere. The simplest model consists of randomly dispersed uniform soft spheres. There are two limiting cases: if the modulus of the soft filler particles is zero, the matrix contains holes (resembling a swiss cheese) and thus becomes softer. Such a material may seem to be only of theoretical interest, but it nevertheless will show how the theory works. On the other hand, in the case of a very large modulus of the filler particles, the Einstein−Smallwood formula will be reproduced.

For uniform soft filler particles with elastic modulus $E_f > E_m$, there are several methods to calculate the intrinsic modulus. For a review see the book of Christensen.[20] The result as given by Jones and Schmitz[19] is

$$[\mu] = 5\frac{1 - E_m/E_f}{2 + 3E_m/E_f} \qquad (3.2)$$

Inserting this into eq 3.1 leads to

$$\frac{E}{E_m} = 1 + \frac{5}{2}\phi\frac{E_f/E_m - 1}{E_f/E_m + {}^3/_2 - \phi(E_f/E_m - 1)} \qquad (3.3)$$

which is shown in Figure 3. This is identical with previous results (as reviewed by Christensen) in first order of ϕ and is valid also for intermediate volume fractions. As these results are already well-known, further discussion will be skipped here.

B. Soft Core/Hard Shell. Now we investigate the case of a particle with a soft core (whose modulus is taken as zero for simplicity) and a shell with modulus E_{shell} always larger than the modulus of the matrix, $E_{shell} \geq E_m$; see Figure 4. The algebraic expression for

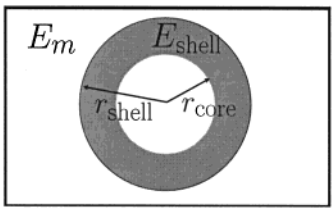

Figure 4. Geometry and nomenclature for core−shell systems.

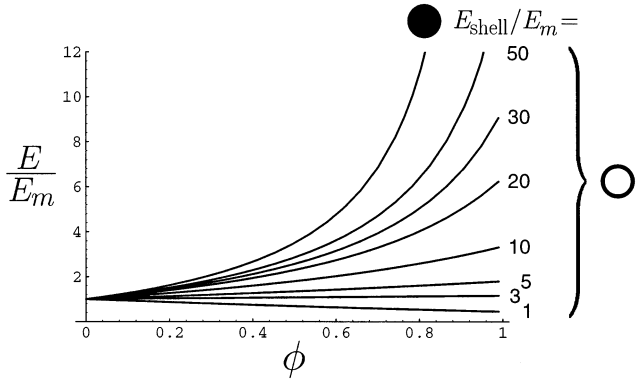

Figure 5. Filler particles with soft core: relative increase of the elastic modulus as a function of filler volume fraction for different values of the ratio $E_{\text{shell}}/E_{\text{m}}$. The ratio between outer and inner shell radius is taken as $^4/_3$; the black circle denotes the limiting case of a totally rigid shell, i.e., $E_{\text{shell}}/E_{\text{m}} \rightarrow \infty$.

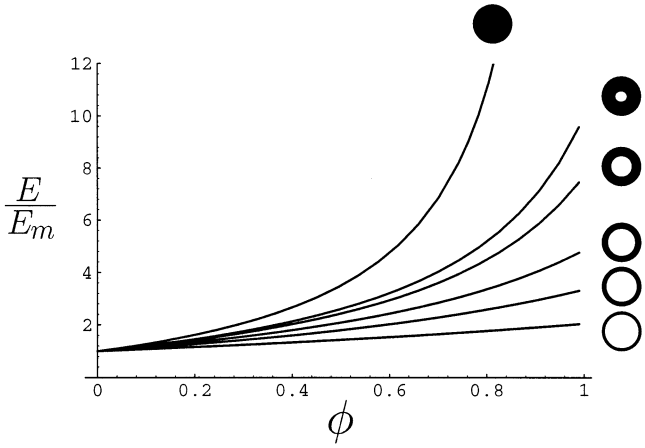

Figure 6. Filler particles with soft core: relative increase of the elastic modulus as a function of filler volume fraction for different values of the ratio between outer and inner shell radius, from bottom to top 6/5, 4/3, 3/2, 2, and ∞. The ratio $E_{\text{shell}}/E_{\text{m}}$ is taken as 10, black-filled circle as above.

the intrinsic modulus is

$$[\mu] = -\frac{5}{3} + \frac{25}{3}\tilde{\mu}\{16\tilde{\mu} + 19 + 5(8\tilde{\mu} - 15)\tilde{r}^3 + (\tilde{\mu} - 1)(-112\tilde{r}^5 + 75\tilde{r}^7 - 19\tilde{r}^{10})\}/\{(3\tilde{\mu} + 2)(16\tilde{\mu} + 19) + (\tilde{\mu} - 1)[50(4\tilde{\mu} + 3)\tilde{r}^3 - 112(3\tilde{\mu} + 2)\tilde{r}^5 + 75(3\tilde{\mu} + 2)\tilde{r}^7 + 38(\tilde{\mu} - 1)\tilde{r}^{10}]\} \quad (3.4)$$

with the abbreviations $\tilde{\mu} = E_{\text{m}}/E_{\text{shell}}$ and $\tilde{r} = r_{\text{shell}}/r_{\text{core}}$.

The resulting effective modulus of the system is depicted in Figures 5 and 6. As expected, the result only depends on the relation between shell and matrix modulus $E_{\text{shell}}/E_{\text{m}}$ and on the relation between outer and inner shell radius (as a measure of shell thickness). For finite $E_{\text{shell}}/E_{\text{m}}$, the whole system remains elastic, i.e., there is no divergence of the effective elastic modulus for ϕ approaching 1. As can be seen from Figure 5, reinforcement takes place only if the stiffness of the shell compensates the softness of the core. This reinforcement condition is presented in a more general way in Figure 7.

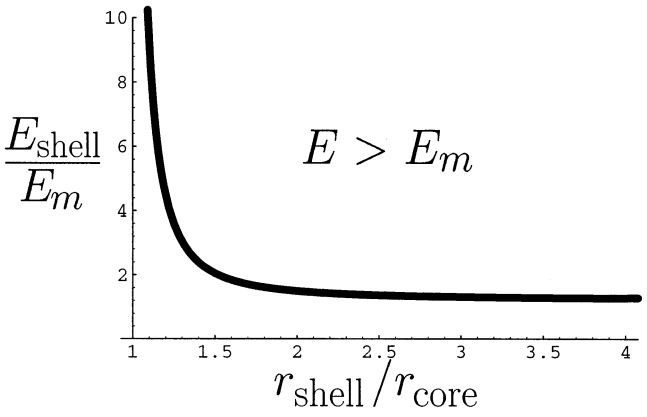

Figure 7. Reinforcement condition for soft core/hard shell systems: reinforcement takes place only for parameters in the upper region $E > E_{\text{m}}$.

C. Hard Core/Soft Shell. In the same way, the intrinsic modulus can be calculated for filler particles with totally rigid core (with infinitely large modulus) and a soft shell. If the shell modulus E_{shell} is assumed to be larger than the matrix modulus E_{m}, this system resembles to lowest order a carbon black filled rubber, where the carbon black particles are surrounded by a bound rubber layer. Here the algebraic expression for the intrinsic modulus reads

$$[\mu] = \frac{5}{2} - 25\tilde{\mu} \times \{(1 - \tilde{r}^3)(8\tilde{\mu} + 19/2) + (\tilde{\mu} - 1)(-42\tilde{r}^3 + 84\tilde{r}^5 - 50\tilde{r}^7 + 8\tilde{r}^{10})\}/\{(3\tilde{\mu} + 2)(16\tilde{\mu} + 19) + (\tilde{\mu} - 1)[-300(\tilde{\mu} + {}^3/_4)\tilde{r}^3 + 168(3\tilde{\mu} + 2)\tilde{r}^5 - 100(3\tilde{\mu} + 2)\tilde{r}^7 + 48(\tilde{\mu} - 1)\tilde{r}^{10}]\} \quad (3.5)$$

with the same abbreviations as above, $\tilde{\mu} = E_{\text{m}}/E_{\text{shell}}$ and $\tilde{r} = r_{\text{shell}}/r_{\text{core}}$.

Figures 8 and 9 show the resulting effective modulus. Most interesting is the strong increase in reinforcement even for small bound rubber thickness (Figure 9). Despite the fractal filler structure as well as many-particle interactions being neglected, the curves have quite realistic features. Unfortunately, for comparison with experimental data still values for the effective bound rubber thickness and strength are lacking. To obtain and insert these seems worthwhile as the theoretical curves do not contain any fit parameters; i.e., all the parameters result from structural filler and matrix properties.

IV. Summary and Outlook

We presented in this paper a simple model for the reinforcement of filled rubbers. To be more specific, the hydrodynamic reinforcement of continuous elastic media containing different filler particles has been investigated. Results were presented as modifications of the celebrated Einstein−Smallwood formula.

Two cases have been studied in detail. The first is the reinforcement by rigid (fractal) aggregates and agglomerates of filler particles. The second case is the reinforcement by randomly dispersed core−shell par-

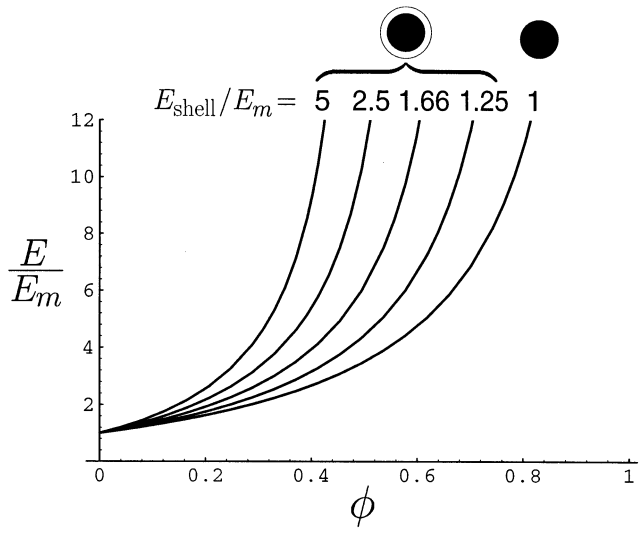

Figure 8. Filler particles with hard core: relative increase of the elastic modulus as a function of filler volume fraction for different values of the ratio E_{shell}/E_m. The ratio between shell and core radius is taken as $^4/_3$.

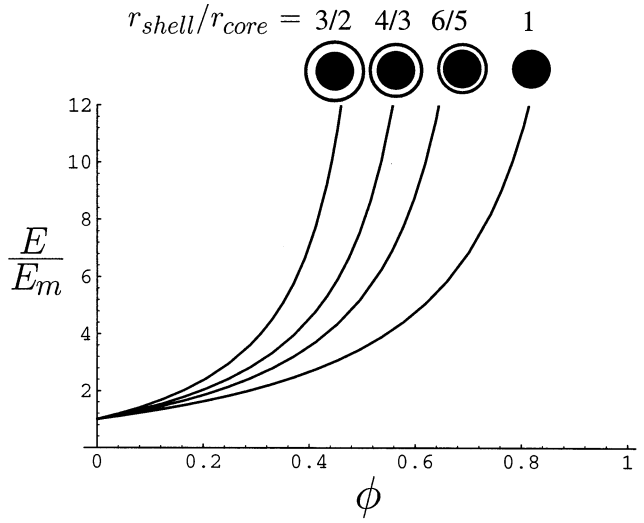

Figure 9. Filler particles with hard core: relative increase of the elastic modulus as a function of filler volume fraction for different values of the ratio between shell and core radius. The ratio E_{shell}/E_m is taken as 2.

ticles containing at least one soft component. The theoretical methods used are extensions of previously developed formalisms on continuum elasticity of composite materials. They differ in detail but are based on the same principles of elastic theory.

Let us briefly discuss the advantages of the model. The first point is that the results obtained are realistic for small as well as intermediate filler concentrations, i.e., they are in accordance with experiments at least qualitatively. For the core−shell systems, we provided exact calculations of intrinsic moduli for various special forms of core−shell elasticity, i.e., soft spheres, hard spheres with soft surfaces, etc. Further important points are that these results contain no fit parameters and that in principle both cases of compressible as well as incompressible media are accessible (only the incompressible case shown here).

In the present paper, we made a first step toward the application of elastic theory to the bound rubber reinforcement in carbon black filled elastomers. Here we treated the cases of clusters and core−shell systems separately with different mathematical tools. As a consequence, we could not obtain realistic results for high filler concentration of core−shell particles, where clustering becomes important. Future work will attempt to combine these two approaches in order to obtain a complete theoretical description of hydrodynamic reinforcement of clusters which are coated by bound rubber material, i.e., carbon black filled elastomers, where structural properties of the filler as well as different rubber phases play a major role. In this connection also the influence of the filler aggregate size distribution will be investigated.

Acknowledgment. Financial support for part of this work by the Ministery of Research, BMBF is gratefully acknowledged. The authors enjoy many ongoing and helpful discussions with Gert Heinrich and Manfred Klüppel.

Appendix A: Effective Medium Theory and Linear Elasticity

In this appendix, we derive the equations for a linear isotropic elastic material with a torsion modulus μ, compression modulus B, Poisson number $\sigma = (3B - 2\mu)/(6B + 2\mu)$, and Youngs modulus $E_m = 2\mu(1 + \sigma)$. Since the material is assumed to be almost incompressible, i.e., B is very large[21]), we may assume that the rubber matrix is effectively incompressible for the purpose in the present paper, i.e., $B \to \infty$ and $\sigma = {}^1/_2$. Furthermore, we assume only small deformations and can therefore compute only the initial modulus; i.e., we ignore finite extensibility effects, as studies extensively earlier[4] which have conformed in the meantime by many experiments.[22−25] The other advantage of a theory for small deformations is that we do not have to worry about the rupture of filler particles from the elastic matrix. These assumptions allow us to extend the theory used already by Cates and Edwards[11] and Freed und Edwards.[12]

We begin with a simple illustration of the theory. The local deformation field of a filled system can be described as

$$\mathbf{u}(\mathbf{r}) = \int \mathrm{d}^3r'\, \mathbf{G}_0(\mathbf{r} - \mathbf{r}')\cdot\mathbf{F}(\mathbf{r}') + \int \mathrm{d}s \int \mathrm{d}^3r'\, \delta(\mathbf{R}(s) - \mathbf{r}')\mathbf{G}_0(\mathbf{r} - \mathbf{r}')\cdot\boldsymbol{\sigma}(s) \quad \text{(A1)}$$

where the Green elastic tensor (Green's function of the unfilled matrix is given by[26]

$$\mathbf{G}_0(\mathbf{r}) = \frac{1}{16\pi\mu|\mathbf{r}|}\left\{\left(\frac{3 - 4\sigma}{1 - \sigma}\right)\mathbf{I} + \frac{\hat{\mathbf{r}}\hat{\mathbf{r}}}{1 - \sigma}\right\} \quad \text{(A2)}$$

The general shape of the filler particles is defined by the parametrization $\mathbf{R}(s)$ and $\mathbf{F}(\boldsymbol{r})$ is the (small) elastic force. The symbol $\mathbf{I}$ denotes the unit matrix, and $\hat{\mathbf{r}}\hat{\mathbf{r}}$ is the matrix defined by the unit vectors $\hat{\mathbf{r}}$ which acts as projection on the direction of $\boldsymbol{r}$; see refs 10 and 26 for details. The essential problem is now to calculate a new form of the Green function $\mathbf{G}$ which contains the effects of the filler particles. Therefore, all effects have to be taken into account: the shape of the filler particles, the spatial distribution of the particles, etc. Effective medium theories have developed detailed formalisms for these calculations, and we can be brief here.

It turns out that it is useful to work in Fourier space. The desired quantity is then given by the aver-

age local deformation,

$$<\mathbf{u}(\mathbf{k})> = \mathbf{G}(\mathbf{k})\cdot\mathbf{F}(\mathbf{k}) \tag{A3}$$

where the Green function of the filled system is given by

$$\mathbf{G}(\mathbf{k}) = \mathbf{G}_0(\mathbf{k}) - \mathbf{G}_0(\mathbf{k})\langle\sum_q \phi^2(\mathbf{k},q)\mathbf{\Delta}(q)\mathscr{G}_0(q)\rangle\mathbf{G}_0(\mathbf{k}) \tag{A4}$$

where the labels q correspond to Fourier components regarding the shape of the particles, i.e., the transformation of $\mathbf{R}(s)$ to their corresponding representation in Fourier components $\mathbf{R}(q)$. The symbol $\mathbf{\Delta}(q)$ is the Fourier transform of the deformation operator and $\mathscr{G}_0(q)$ the general Green function of the shape of the filler particle. Thus, we have

$$\sum_{q'}(\delta_{qq'}\mathbf{I} + [q|\mathbf{G}_0|\ q']\mathbf{\Delta}(q'))\mathscr{G}_0(q) = \mathbf{I} \tag{A5}$$

The reinforcement effects can then be written on a general basis as

$$\mathbf{G}(\mathbf{k}) = \mathbf{G}_0(\mathbf{k}) - \mathbf{G}_0(\mathbf{k})\,\langle\mathbf{T}\rangle\mathbf{G}_0(\mathbf{k}) \tag{A6}$$

where $\langle\mathbf{T}\rangle$ contains the information on the filler particles and can be written as

$$\mathbf{T} = \phi\Delta\mathscr{G}_0\phi = \sum_q \phi^2(\mathbf{k}, q)\Delta(q)\mathscr{G}_0(q) \tag{A7}$$

The quantity ϕ contains all information on shape (and elasticity) of the filler particles.

These approaches can be generalized to many filler particles. The natural generalization of eq A6 is given by

$$\mathbf{G} = \mathbf{G}_0 - \mathbf{G}_0\sum_{\alpha=1}^{N}\langle\mathbf{T}^\alpha\rangle\mathbf{G}_0 + \mathbf{G}_0\sum_{\alpha\neq\beta}\langle\mathbf{T}^\alpha\mathbf{G}_0\mathbf{T}^\beta\rangle\mathbf{G}_0 - \mathbf{G}_0\sum_{\alpha\neq\beta\gamma\neq\beta}\sum\langle\mathbf{T}^\alpha\mathbf{G}_0\mathbf{T}^\beta\mathbf{G}_0\mathbf{T}^\gamma\rangle\mathbf{G}_0 + \ldots \tag{A8}$$

where α is the particle number. Note that eq A8 is of the Dyson type, well-known in quantum field theory. Indeed the methods developed there are useful to resolve the present problem at least in some reasonable approximations. It is most convenient to recast it in the more comfortable form in terms of the geometric series

$$\mathbf{G}^{-1} \approx (\mathbf{G}_0 - \mathbf{G}_0\bar{\mathbf{T}}\mathbf{G}_0 + \mathbf{G}_0\bar{\mathbf{T}}\mathbf{G}_0\bar{\mathbf{T}}\mathbf{G}_0 - \ldots)^{-1} = \mathbf{G}_0{}^{-1} + \bar{\mathbf{T}} \tag{A9}$$

As long as the filler particles do not overlap and do not interact with each other, the solution of eq A8 yields a simple generalization of the Einstein−Smallwood law. If the particles overlap, interactions may screen themselves, as is well-known from the theory of concentrated polymer solutions.[27] Indeed it turns out here that similar methods such as a "self-consistent screening approximation" resolves the problem of many filler particles above their overlap concentration. This will become obvious, if the filler particles are to interpenetrate each other, such as fractallike aggregates. Then the reinforcement is given not only by the volume effect but also by their overlap-induced additional reinforcement. The theory of Green functions allows to compute the corresponding self-energy Σ in terms of the irreducible diagrams in the matrix $\bar{\mathbf{T}}$. The self-consistent screening model ends up in the set of equations which have to be solved self-consistently and simultaneously

$$\mathbf{G}^{-1}(\mathbf{k}) = \mathbf{G}_0{}^{-1}(\mathbf{k}) + \boldsymbol{\sigma}(\mathbf{k}) \tag{A10}$$

$$\sum(\mathbf{k}) = N\langle\sum_q \phi^2(\mathbf{k}, q)\Delta(q)\mathscr{G}(q)\rangle \tag{A11}$$

$$\mathbf{I} = \sum_{q'}(\delta_{qq'}\mathbf{I} + [q|\mathbf{G}|q']\Delta(q'))\mathscr{G}(q) \tag{A12}$$

The most interesting effect is given by the mode dependence of the effective screening, which shows that the screening of the elastic interaction is only relevant for small length scales, whereas on large scales the elasticity becomes reinforced. We may then approximate the screened elastic Green function by

$$G(\mathbf{k}) \sim \frac{1}{\mu(k^2 + \xi^{-2})} \tag{A13}$$

where we introduced a usual screening length as ξ. In the following, we need to compute the screening lengths as a function of filler shape and concentration. The next step is then to evaluate the corresponding properties for filler agglomerates, i.e., to compute these functions with respect to the properties of the filler particle. This is outlined in the main text.

References and Notes

(1) Torquato, S. *Random heterogeneous materials*; Springer, Berlin, 2002.
(2) Huber, G.; Vilgis, T. A. *Kautsch. Gummi Kunstst.* **1999**, *52*, 102.
(3) Vilgis, T. A.; Heinrich, G. *Kautsch. Gummi Kunstst.* **1995**, *48*, 323.
(4) Edwards, S. F.; Vilgis, T. A. *Rep. Prog. Phys* **1988**, *216*, 327.
(5) Smallwood, H. M. *J. Appl. Phys.* **1944**, *15*, 758.
(6) Guth, E.; Gold, O. *Phys. Rev.* **1938**, *53*, 322. Guth, E. *J. Appl. Phys.* **1945**, *16*, 20.
(7) Klüppel, M.; Heinrich, G. *Rubber Chem. Technol.* **1995**, *68*, 623.
(8) Medalia, A. I. *Rubber Chem. Technol.* **1978**, *51*, 437.
(9) Bunde, A.; Havlin, S., Eds. *Fractals and Disordered Systems*; Springer-Verlag: Berlin, 1991.
(10) Jhon, M. S.; Metz, R. J.; Freed, K. F. *J. Stat. Phys.* **1988**, *52*, 1325.
(11) Cates, M. E.; Edwards, S. F. *Proc. R. Soc. A* **1984**, *395*, 9.
(12) Freed, K. F.; Edwards, S. F. *J. Chem. Phys.* **1974**, *61*, 3626. Edwards, S. F.; Freed, K. F. *J. Chem. Phys.* **1974**, *61*, 1189.
(13) Nelson, D.; Piran, T.; Weinberg, S.; Eds.; *Statistical mechanics of membranes and surfaces*; World Scientific: Singapore, 1989.
(14) Vilgis, T. A. *Phys. Rep.* **2000**, *336*, 167.
(15) Vilgis, T. A. *Physica A* **1988**, *153*, 341.
(16) Haronska, P.; Vilgis, T. A. *J. Chem. Phys.* **1995**, *102*, 6586.
(17) Heinrich, G.; Klüppel, M. *Adv. Polym. Sci.* **2002**, *160*, 2.
(18) Felderhof, B. U.; Iske, P. L. *Phys. Rev. A* **1992**, *45*, 611.
(19) Jones, R. B.; Schmitz, R. *Physica A* **1983**, *122*, 105.
(20) Christensen, R. M. *Mechanics of composite materials*; Krieger: Malabar, India, 1991.
(21) Treloar, L. R. G. *The physics of rubber elasticity*; Clarendon Press: Oxford, England, 1975.
(22) Uyarama, K.; Kawamura, T.; Kohjiya, S. *Macromolecules* **2001**, *34*, 8261.
(23) Meissner, B.; Matejka, L. *Polymer* **2002**, *43*, 3803.
(24) Sweeney, J. *Comput. Theor. Polymer Sci* **1999**, *9*, 27.
(25) Buckley, C. P.; Jones, D. C. *Polymer* **1995**, *36*, 3301.
(26) Landau, L. D.; Lifschitz, E. M. *Elastizitätstheorie*; Akademie-Verlag: Berlin, 1983.
(27) Doi, M.; Edwards S. F. *The theory of polymer dynamics*; Oxford Clarendon Press: Oxford, England, 1986.

MA0208887